

X-ray Diffraction Analysis of Geometry Changes upon Excitation: The Ground-State and Metastable-State Structures of $K_2[Ru(NO_2)_4(OH)(NO)]$

Dmitry V. Fomitchev and Philip Coppens*

Chemistry Department, Natural Sciences Complex, State University of New York at Buffalo, Buffalo, New York 14260-3000

Received June 14, 1996[⊗]

The structure of the laser-light-induced metastable state MS_1 of the $[Ru(NO_2)_4(OH)(NO)]^{2-}$ anion in $K_2[Ru(NO_2)_4(OH)(NO)]$ was determined by X-ray analysis at 50 K of a crystal with a 16% excited-state population. Results of an independent determination of the ground-state structure were used in the analysis. The most pronounced geometrical change upon excitation was an increase of the Ru–(NO) distance by 0.097(11) Å, significantly larger than the change of the corresponding distance in sodium nitroprusside (Pressprich, M. R.; White, M. A.; Vekhter, Y.; Coppens, P. *J. Am. Chem. Soc.* **1994**, *116*, 5233–5238). A decrease in the $\angle Ru-(N-O)$ angle from 174.0(2) to 169(1)[°] was observed. The diffraction results provide evidence that the photoinduced state MS_1 of the transition metal nitrosyl complexes is a linkage isomer in which the NO group is attached to the metal atom through the oxygen, instead of through the nitrogen atom, rather than an electronic excited state as reported previously.

Introduction

Several nitrosyl complexes of transition metals were recently found to have light-induced metastable states with very long lifetimes at reduced temperatures.¹ The most extensively studied among these is sodium nitroprusside or SNP, $Na_2[Fe(CN)_5(NO)] \cdot 2H_2O$, for which two light-induced metastable electronic states (MS_1 and MS_2) having different decay temperatures were observed. The nature of the excited states has been explored by different physical methods such as differential scanning calorimetry (DSC), infrared and Raman spectroscopy, Mössbauer spectroscopy, and X-ray and neutron diffraction.^{2–8} However, the exact electronic configurations of MS_1 and MS_2 , and the origin of their unusually long lifetimes at low temperatures are still a matter of controversy. Two different models have been proposed for the first metastable state of sodium nitroprusside. According to the first model,⁷ MS_1 is a relaxed derivative arising from the metal-to-ligand charge transfer from the highest occupied $2b_2$ (d_{xy}) orbital to a $7e$ (π^*NO) orbital, corresponding to the transition $...6e(d_{xz}, d_{yz})^4 2b_2(d_{xy})^2 (^1A_1) \rightarrow 6e(d_{xz}, d_{yz})^4 2b_2(d_{xy}) 7e(\pi^*NO) (^1E)$, while the alternative description⁹ is based on a transition to the $5a_1(d_z^2)$ orbital, leading to the $...6e(d_{xz}, d_{yz})^4 2b_2(d_{xy}) 5a_1(d_z^2) (^1B_2)$ electronic configuration.

Similar long-lived states are formed upon irradiation of analogous nitrosyl complexes with Ru or Os,^{6,10} with different cations and different ligands. Questions about the geometrical configuration of these complexes in the excited state and the influence of ligands equatorial and axial to the nitrosyl group on the population of the excited states and about the decay temperatures remain unanswered.

Two light-induced long-lived metastable electronic states have been reported for $K_2[Ru(NO_2)_4(OH)(NO)]^{10}$ and characterized by IR spectroscopy and differential scanning calorimetry. As in the other complexes, the NO ligand is the one most affected by the excitation; the stretching vibration frequencies of NO downshift by 114 and 263 cm^{-1} , while the stretching frequencies of the trans ligand (OH) decrease by only 29 and 61 cm^{-1} in MS_1 and MS_2 , respectively. The decay temperatures for MS_1 are the same for both $K_2[Ru(NO_2)_4(OH)(NO)]$ and SNP (≈ 200 K) but differ for MS_2 , for which the values are 166 K and 150 K, respectively. The reported maximum populations of the excited states due to direct excitation with ≈ 450 nm light are only 16% for MS_1 and 2% for MS_2 in the Ru complex *vs* 50% and 11%, respectively, for SNP.

Though the spectroscopic data are a sensitive probe of excitation, they only give indirect information on the geometry changes upon excitation. In this paper we present results on the geometry of the $[Ru(NO_2)_4(OH)(NO)]^{2-}$ anion in the first metastable electronic state as determined by single-crystal X-ray diffraction.

Experimental Section

Sample Preparation. $K_2[Ru(NO_2)_4(OH)(NO)]$ was obtained from $RuCl_3$ by the method described in ref 11 and recrystallized from a water solution. The samples for differential scanning calorimetry measurements were ground into thin plates with dimensions $3.0 \times 1.8 \times 0.45$ and $3.2 \times 1.1 \times 0.5$ mm, with the directions of the crystallographic *b*- and *a* axes, respectively, perpendicular to the plane of the plate. For the collection of X-ray data on the partially excited crystal, a specimen with the *b* axis perpendicular to the plane of the plate was mounted on an aluminum pin, with the plane of the plate perpendicular to the long

* Author to whom correspondence should be addressed.

[⊗] Abstract published in *Advance ACS Abstracts*, November 1, 1996.

- (1) Zöllner, H.; Krasser, W.; Woike, Th. *Chem. Phys. Lett.* **1989**, *161*, 497–501.
- (2) Woike, Th.; Krasser, W.; Zöllner, H.; Kirchner, W.; Haussühl, S. *Z. Phys. D* **1993**, *25*, 351–356.
- (3) Rüdinger, M.; Schefer, J.; Vogt, T.; Woike, Th.; Haussühl, S.; Zöllner, H. *Physica B* **1992**, *180/181*, 293–298.
- (4) Pressprich, M. R.; White, M. A.; Vekhter, Y.; Coppens, P. *J. Am. Chem. Soc.* **1994**, *116*, 5233–5238.
- (5) Carducci, M.; Pressprich, M. R.; Coppens, P. To be published.
- (6) Güida, J. A.; Piro, O. E.; Aymonino, P. *J. Inorg. Chem.* **1995**, *34*, 4113–4116.
- (7) Woike, Th.; Krasser, W.; Bechthold, P. S.; Haussühl, S. *Solid State Commun.* **1983**, *45* (6), 499–502.
- (8) Woike, Th.; Kirchner, W.; Kim, H.; Haussühl, S.; Rusanov, V.; Angelov, V.; Ormandjiev, S.; Bonchev, V.; Schroeder, A. N. *F. Hyperfine Interact.* **1993**, *77*, 265–275.
- (9) Terrile, C.; Nascimento, O. R.; Moraes, I. J.; Castellano, E. E.; Piro, O. E.; Guida, J. A.; Aymonino, P. *J. Solid State Commun.* **1990**, *73*, 481–486.

(10) Woike, Th.; Haussühl, S. *Solid State Commun.* **1993**, *86*, 333–337.

(11) Fletcher, J. M.; Jenkins, I. L.; Lever, F. M.; Martin, F. S.; Powell, A. R.; Todd, R. *J. Inorg. Nucl. Chem.* **1955**, *1*, 378–401.

axis of the pin. This mounting allows the polarization direction of the light to be parallel to the crystallographic c axis, which the DSC experiments described below indicate to yield the highest population of MS_1 . The metastable states were generated by irradiating the crystal at 50 K for 5 h with $\lambda = 454$ nm light from an Ar^+ laser, with a power of 360 mW/cm², and light propagation along the b direction. Once a steady-state excited state population was obtained, as judged by the intensities of excitation-sensitive reflections, the laser was switched off and the crystal was warmed to 166 K, maintained at this temperature for 5 min to eliminate the MS_2 , and then cooled back to 50 K.

DSC Experiment. The amount of heat released during thermally stimulated decay of the metastable electronic states was measured by a Perkin-Elmer differential scanning calorimeter DSC7. The crystals were heated at a constant rate of 4 K/min, while the enthalpy supplied to effect the heating was being monitored. A window was installed in the calorimeter enclosure, to allow laser irradiation of the specimen at 110 K.

X-ray Data Collection. Four sets of X-ray intensities were collected on a HUBER D-511.1 four-circle diffractometer using graphite-monochromated Mo $K\alpha$ radiation from a Rigaku Corp. rotating anode ROTAFLEX RU-200b generator (60 kV, 90 mA). The diffractometer was equipped with a two-stage closed-cycle helium Displex CT211 cryostat, manufactured by Air Products and Chemicals, Inc., mounted as described elsewhere.¹² A half-cylinder-shaped ($r = 90$ mm) imaging plate (IP) holder was mounted on the diffractometer coaxially with the φ axis. This construction allows reflections with 2θ values up to 110° to be measured.

All data were collected at 50 K. During the experiment the temperature was monitored with a silicon diode thermometer manufactured by Scientific Instruments, Inc. Before the experiment, the temperature reading was checked against the real temperature at the position of a crystal by observation of the phase transitions of KH_2PO_4 and $TbVO_4$, which occur at 122 K and 33 K, respectively.^{13,14}

First, data sets were collected on ground-state and mixed ground-state/first-excited-state crystals using a scintillation counter as the intensity detector. This experiment will not be further reported here, as its results are in full agreement with those of the second experiment, in which more extensive data sets were collected using imaging plates as detectors. Data were collected on the crystal in the ground state and mixed ground state/first-excited electronic state. An "antiscatter device" was introduced into the vacuum chamber to shield the imaging plate from the scattering by the walls of the vacuum chamber.¹⁵ FUJI HR-IIIN imaging plates and a FUJI BAS2000 scanner and visualization software were used. Data were collected with 8° φ oscillations of 4 min exposure time each. A slight but statistically significant increase of the b -axis length from 12.348(1) Å in the ground state to 12.353(1) Å in the laser-saturated excited-state was observed. Crystal data and X-ray data collection details are summarized in Table 1.

Data Reduction. The integration of the IP data was performed with the program HIPPO based on the "seed-skewness" method.¹⁶ The programs ABSORB,¹⁷ modified for use with IP data, and SORTAV^{18,19} were used for absorption correction and for merging of the reflections, respectively.

The efficiency of the IP method permits a considerable redundancy in the data collection and allows the scaling of the statistical standard deviations using the distribution of equivalent measurements. If σ' is the scaled standard deviation and σ the statistical standard deviation

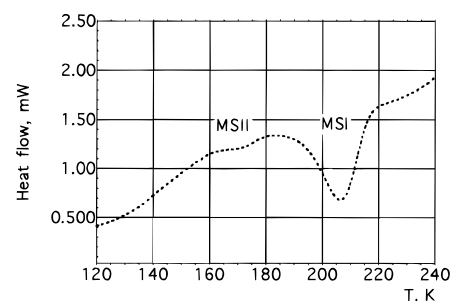


Figure 1. Heat flow vs temperature, for a constant temperature increase of 4 K/min, of a previously laser-irradiated single-crystal sample of $K_2[Ru(NO_2)_4(OH)(NO)]$.

Table 1. Experimental Data for $K_2[Ru(NO_2)_4(OH)(NO)]$

	ground state	MS_1 /ground state
space group	$P2_1/a$	$P2_1/a$
temp (K)	50(2)	50(2)
a (Å)	12.380(1)	12.381(1)
b (Å)	12.348(1)	12.353(1)
c (Å)	6.926(1)	6.924(1)
β (deg)	93.32(1)	93.27(1)
V (Å ³)	1057.0	1057.3
Z	4	4
d_{calc} (g/cm ³)	2.578	2.578
abs coeff (cm ⁻¹)		23.01
transm coeff		0.848–0.707
crystal dimens (mm)		$0.15 \times 0.125 \times 0.1$
radiation wavelength (Å)	0.7107	0.7107
range of $(\sin \theta)/\lambda$ (Å ⁻¹)	0.08–1.03	0.08–1.03
h, k, l : lower limit; upper limit	-22, -10, -12; 16, 14, 11	-22, -10, -12; 22, 14, 12
no. of rflns meas	6688	8668
no. of symm-unique rflns	3010	3219
no. of rflns with $F > 4\sigma(F)$	2789	3013
merging factor R (%)	2.3	2.2
$R(F), R_w(F)$ (%)	2.6, 2.9	2.5, 2.8

before scaling

$$\sigma' = \sigma[Q(I, (\sin \theta)/\lambda)]$$

where I is the intensity and Q a quadratic function fitted to the ratio of the rms deviation among repeated measurements and the esd of the average of the repeated measurements.^{18,19} In the subsequent least-squares refinements, the function $\sum w(|F_o| - k|F_c|)^2$ was minimized with $w = 1/\sigma'^2(F_o)$. All least-squares refinements were done with the SDS structure refinement package.²⁰

Results

DSC Experiment. The DSC curve indicating the thermal decay of MS_1 and MS_2 in a single crystal of $K_2[Ru(NO_2)_4(OH)(NO)]$ is shown in Figure 1. With an energy difference between the MS_1 and the ground-state level of $K_2[Ru(NO_2)_4(OH)(NO)]$ of 1 eV,¹⁰ the amount of heat released during the thermal decay of MS_1 corresponds to a population of 16%, in agreement with the value reported in ref 10. It should be noted that the populations of MS_1 and MS_2 are dependent on the polarization direction of the incident light. In our experiments three different polarization directions $El|c$, $kl|b$; $El|a$, $kl|b$; and $El|b$, $kl|a$ were examined. While the light exposure was approximately the same in all three cases, the MS_1 populations were different at 16, 10, and 8%, respectively.

Structure of the Ground State. Starting positions for all atoms were taken from the literature.²¹ The ground-state

- (12) Henriksen, K.; Larsen, F. K.; Rasmussen, S. E. *J. Appl. Crystallogr.* **1986**, *19*, 390–394. Graafma, H.; Sagerman, G.; Coppens, P. *J. Appl. Crystallogr.* **1991**, *24*, 961–962.
- (13) Kobayashi, J.; Uesu, Y.; Mizutani, I.; Enomoto, Y. *Phys. Status Solidi A* **1970**, *3*, 63–69.
- (14) Will, G.; Gobel, H.; Sampson, C. F.; Forsyth, J. B. *Phys. Lett.* **1971**, *38A*, 207–208.
- (15) Darovsky, A.; Bolotovskiy, R.; Coppens, P. *J. Appl. Crystallogr.* **1994**, *27*, 1039–1040.
- (16) Bolotovskiy, R.; White, M. A.; Darovsky, A.; Coppens, P. *J. Appl. Crystallogr.* **1993**, *28*, 86–95. Bolotovskiy, R. Imaging Plate Area-Detectors in Accurate Crystallographic Studies. Ph.D. Thesis, State University of New York at Buffalo, May 1996.
- (17) De Titta, G. T. *J. Appl. Crystallogr.* **1985**, *18*, 438–440.
- (18) Blessing, R. H. *Crystallogr. Rev.* **1987**, *1*, 3–58.
- (19) Blessing, R. H. *J. Appl. Crystallogr.* **1989**, *22*, 396–397.

- (20) Petricek, V. *SDS94: System of programs for structure solution*; Institute of Physics: Praha, Czech Republic, 1994.
- (21) Butman, L. A.; Khodashova, T. S.; Minacheva, L. K.; Tayukin, V. I. *Zh. Strukt. Khim.* **1964**, *5* (2), 250–256.

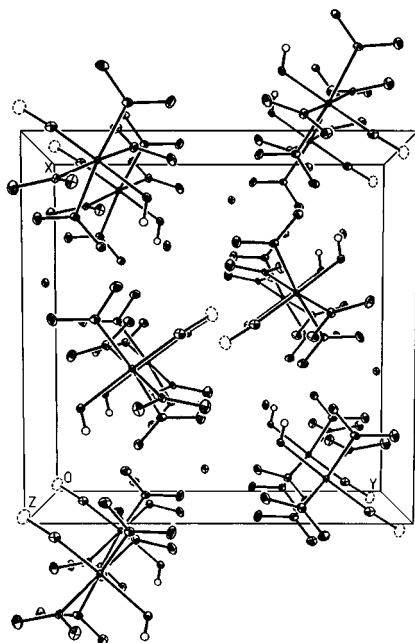


Figure 2. Packing diagram of the structure. 50% probability ellipsoids are shown.

Table 2. Atomic Fractional Coordinates and Isotropic Thermal Parameters for Ground-State $K_2[Ru(NO_2)_4(OH)(NO)]$ at 50 K

atom	<i>x</i>	<i>y</i>	<i>z</i>	<i>U</i> _{iso} (Å ²)
Ru	0.09626(1)	0.20951(1)	0.25470(2)	0.00352(5)
K(1)	0.22259(4)	0.86108(4)	0.26865(7)	0.0081(1)
K(2)	0.12346(3)	0.53685(4)	0.24507(6)	0.0063(1)
N(1)	0.0123(1)	0.0955(2)	0.2088(3)	0.0072(5)
N(2)	0.2216(1)	0.1430(2)	0.1022(3)	0.0069(5)
N(3)	-0.0227(1)	0.2893(2)	0.4027(3)	0.0059(5)
N(4)	0.0413(1)	0.2858(2)	-0.0024(2)	0.0063(5)
N(5)	0.1585(1)	0.1298(2)	0.5058(3)	0.0060(5)
O(1)	0.1895(1)	0.3302(1)	0.3268(2)	0.0067(4)
O(2)	0.2236(1)	0.0456(1)	0.0623(2)	0.0093(4)
O(3)	0.2935(1)	0.2036(1)	0.0464(2)	0.0089(4)
O(4)	0.1787(1)	0.0314(2)	0.4945(3)	0.0109(5)
O(5)	0.1773(1)	0.1778(2)	0.6601(2)	0.0096(5)
O(6)	-0.0966(1)	0.2357(2)	0.4709(2)	0.0095(4)
O(7)	-0.0214(1)	0.3891(2)	0.4206(3)	0.0124(5)
O(8)	-0.0189(1)	0.2347(2)	-0.1196(3)	0.0097(4)
O(9)	0.0690(1)	0.3792(2)	-0.0422(3)	0.0112(5)
O(10)	-0.0365(2)	0.0171(2)	0.1912(3)	0.0141(5)
H	0.252(3)	0.315(3)	0.300(5)	0.014(11)

structure was refined by full-matrix least squares (LS) with anisotropic temperature parameters for all non-H atoms, to give final agreement factors of $R = 0.026$, $R_w = 0.029$. Final positional and isotropic temperature parameters obtained are listed in Table 2, while bond lengths and angles from both experiments are presented in Table 4. The highest residual peak in the difference Fourier synthesis is $0.32 \text{ e}/\text{\AA}^3$, 0.6 \AA from the position of the potassium ion, and the deepest minimum is $-0.4 \text{ e}/\text{\AA}^3$, 0.7 \AA from the position of the ruthenium atom. A packing diagram of the structure is presented in Figure 2, while the numbering of the atoms and the anion geometry are given in Figure 3.

Structure of the First Metastable State. Starting positions for all atoms were taken from the ground-state structure. In the first stage only the scale factor was refined to give the agreement factors $R = 0.046$, $R_w = 0.050$. Subsequent difference Fourier maps showed several new residual features, ranging from a maximum of $4.4 \text{ e}/\text{\AA}^3$ to a minimum of $-3.84 \text{ e}/\text{\AA}^3$, both 0.25 \AA from the position of the Ru atom (Figure 4). Similar but smaller features are found near the other atoms of

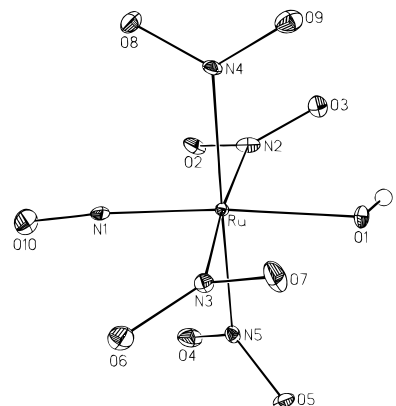


Figure 3. Geometry of the anion and numbering of the atoms. Ellipsoids are as in Figure 2.

the anion. They are evidence for the occurrence of structural changes induced by the laser light.

Refinement of the parameters of the metastable state MS_1 requires the inclusion of both ground-state and excited-state components, since only a portion of the molecules in the crystal are excited. The appropriate structure factor expression is

$$F = (1 - P)F_{gs, [Ru(NO_2)_4(OH)(NO)]^{2-}} + PF_{ms, [Ru(NO_2)_4(OH)(NO)]^{2-}} + F_{rest}$$

where gs and ms represent the ground and metastable states, respectively, P is the metastable-state population, and the subscript "rest" represents the potassium ions, which are not involved in the excitation.

To obtain the structure of the excited state, the ground-state $[Ru(NO_2)_4(OH)(NO)]^{2-}$ anion was assigned a population of 84%, based on the DSC experiments, and treated as a rigid body which was allowed to rotate around three perpendicular axes. Positional parameters of the remaining 16% of the atoms constituting the excited anion were allowed to refine. In this refinement the temperature factors of the excited-state atoms were fixed at their ground-state values. Positional and thermal parameters of the cations were also included in the refinement. The structure was refined to $R = 0.025$ and $R_w = 0.028$. The highest remaining peak in the difference Fourier synthesis was $0.55 \text{ e}/\text{\AA}^3$, and the deepest minimum was $-0.53 \text{ e}/\text{\AA}^3$. Correlation coefficients did not exceed 0.7 in the last cycle of the refinement. Final positional and thermal parameters of the excited-state structure from this refinement are listed in Table 3. The bond lengths and angles of the ground- and excited-state structures are summarized in Table 4. Changes upon irradiation are illustrated in Figure 5.

Because of high correlations between the ground-state population of the rigid body and the positional parameters of the excited state Ru atom, it is not possible to determine the population of MS_1 in the mixed-state crystal by least-squares refinement.

Discussion

Geometry Changes. Our results on the geometry of the $[Ru(NO_2)_4(OH)(NO)]^{2-}$ anion in the ground state at 50 K are in good agreement with those from the previous room-temperature study of $Na_2[Ru(NO_2)_4(OH)(NO)] \cdot 2H_2O$.²² Examination of the Cambridge Structural Data Base shows the Ru-N(1) and N(1)-O(10) distances and Ru-N(1)-O(10) angle to be in the typical range for ruthenium mononitrosyl complexes.

(22) Blake, A. J.; Gould, R. O.; Johnson, B. F. G.; Parisini, E. *Acta Crystallogr.* **1992**, *C48*, 982-984.

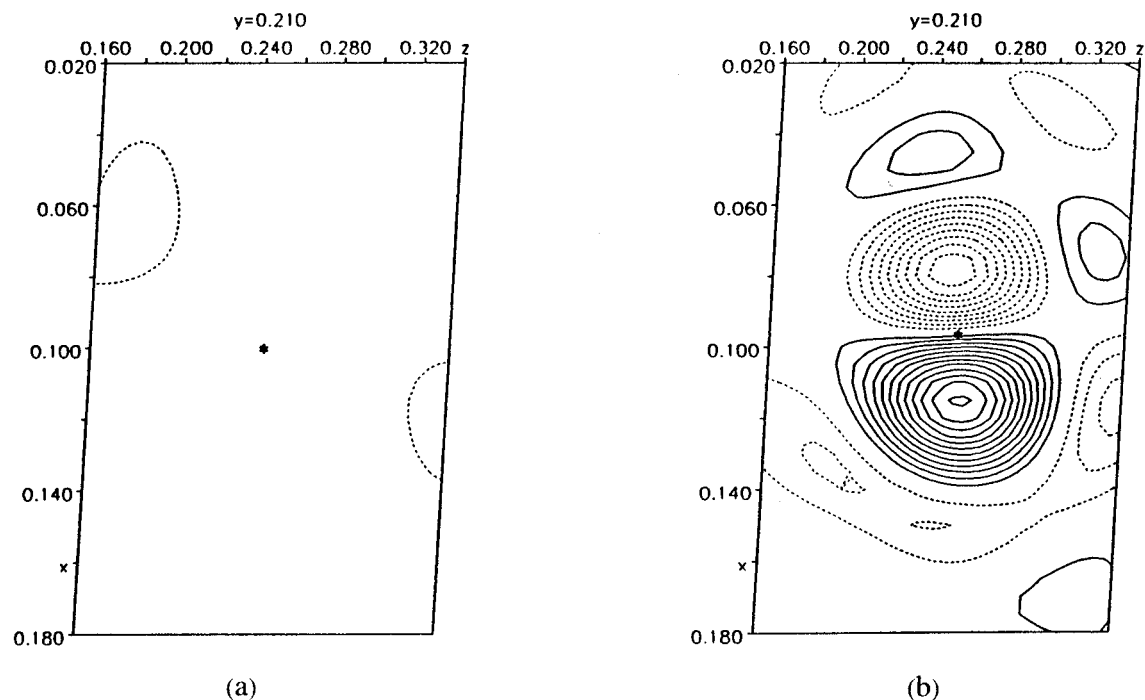


Figure 4. Difference Fourier map in a section parallel to the *ac* plane through the position of the Ru atom (indicated by *). Contour levels are at $0.4 e \text{ \AA}^{-3}$; negative contours, dotted; zero contour, omitted. Panel a shows the ground state and panel b shows the excited state of the crystal with the anion based on ground state parameters subtracted.

Table 3. Atomic Fractional Coordinates and Isotropic Thermal Parameters for the First-Excited-State $\text{K}_2[\text{Ru}(\text{NO}_2)_4(\text{OH})(\text{NO})]$ at 50 K

atom	<i>x</i>	<i>y</i>	<i>z</i>	$U_{\text{iso}}(\text{\AA}^2)$
Ru	0.10051(6)	0.21115(7)	0.2557(1)	<i>a</i>
K(1)	0.22218(3)	0.86093(3)	0.26825(6)	0.0082(1)
K(2)	0.12343(3)	0.53671(3)	0.24479(6)	0.0063(1)
N(1)	0.0104(9)	0.0917(9)	0.2107(16)	<i>a</i>
N(2)	0.2216(8)	0.1423(9)	0.107(1)	<i>a</i>
N(3)	-0.0168(7)	0.2938(9)	0.403(1)	<i>a</i>
N(4)	0.0438(8)	0.287(1)	-0.003(1)	<i>a</i>
N(5)	0.1593(8)	0.131(1)	0.504(1)	<i>a</i>
O(1)	0.1950(7)	0.3311(8)	0.322(1)	<i>a</i>
O(2)	0.2190(9)	0.0422(9)	0.067(1)	<i>a</i>
O(3)	0.2963(7)	0.197(1)	0.046(1)	<i>a</i>
O(4)	0.1744(9)	0.0314(9)	0.500(2)	<i>a</i>
O(5)	0.1857(7)	0.179(1)	0.659(1)	<i>a</i>
O(6)	-0.0925(7)	0.237(1)	0.468(1)	<i>a</i>
O(7)	-0.0170(9)	0.390(1)	0.423(2)	<i>a</i>
O(8)	-0.0162(7)	0.231(1)	-0.119(1)	<i>a</i>
O(9)	0.0699(9)	0.378(1)	-0.049(2)	<i>a</i>
O(10)	-0.033(1)	0.011(1)	0.204(2)	<i>a</i>
H	<i>a</i>	<i>a</i>	<i>a</i>	<i>a</i>

^a Parameter kept constant at ground-state value.

Changes which occur in the geometry of the anion upon excitation to MS_1 are comparable to those found for the $[\text{Fe}(\text{CN})_5(\text{NO})]^{2-}$ anion. The elongation of the Ru–N(1) bond by 0.097(11) Å is twice that for SNP, for which we found values of 0.049(8)⁴ and 0.053(6) Å.⁵ As mentioned earlier, the excited-state population could not be refined directly from the diffraction data. If the excited-state population would be significantly different from the 16% determined by DSC, the Ru–N(1) bond length is affected, as confirmed by a series of refinements with different (constant) excited-state populations. In Figure 6 the Ru–N(1) bond length is plotted *vs* the excited-state population used in the refinement. As can be seen from this graph, a large Ru–N(1) bond elongation can be the result of underestimation of the population of MS_1 . However, a change in the Ru–N(1) distance of 0.05 Å, as observed for Fe–N in SNP, would correspond to a population of 36%, which can be ruled out.

Table 4. Bond Lengths (Å) and Angles (deg) for Ground-State and MS_1 $\text{K}_2[\text{Ru}(\text{NO}_2)_4(\text{OH})(\text{NO})]$ at 50 K

bond	ground state	excited state	
		Ru–N–O	Ru–O–N
Ru–X(1) ^a	1.768(2)	1.865(11)	1.868(9)
Ru–N(2)	2.095(2)	2.051(11)	2.047(11)
Ru–N(3)	2.089(2)	2.088(10)	2.084(10)
Ru–N(4)	2.093(2)	2.110(11)	2.107(11)
Ru–N(5)	2.105(2)	2.079(11)	2.079(11)
Ru–O(1) (OH)	1.933(2)	1.927(10)	1.923(10)
N(1)–O(10) (NO)	1.144(3)	1.137(17)	1.130(17)
N(2)–O(2)	1.234(2)	1.268(16)	1.283(17)
N(2)–O(3)	1.242(3)	1.239(15)	1.233(15)
N(3)–O(6)	1.244(2)	1.272(15)	1.273(15)
N(3)–O(7)	1.239(3)	1.194(17)	1.200(17)
N(4)–O(8)	1.242(2)	1.268(15)	1.260(16)
N(4)–O(9)	1.239(3)	1.209(18)	1.221(18)
N(5)–O(4)	1.244(3)	1.243(18)	1.236(18)
N(5)–O(5)	1.232(3)	1.252(15)	1.251(15)
O(1)–H	0.83(4)		

angle	ground state	excited state	
		Ru–N–O	Ru–O–N
Ru[N(1)–O(10)]	174.0(2)	169(1)	169(1)
Ru–O(1)–H	108(2)		
X(1)–Ru–N(2)	92.42(8)	92.1(5)	92.2(4)
X(1)–Ru–N(3)	92.26(8)	92.4(5)	92.4(4)
X(1)–Ru–N(4)	92.68(8)	92.6(5)	92.5(5)
X(1)–Ru–N(5)	87.68(8)	86.5(5)	86.2(5)
X(1)–Ru–O(1)	175.27(8)	175.8(5)	175.4(4)
N(2)–Ru–O(1)	89.07(7)	89.2(4)	89.1(4)
N(3)–Ru–O(1)	86.41(7)	86.5(4)	86.5(4)
N(4)–Ru–O(1)	91.86(7)	91.5(4)	92.0(4)
N(5)–Ru–O(1)	87.85(7)	89.5(4)	89.3(4)
O(2)–N(2)–O(3)	119.6(2)	118(1)	118(1)
O(6)–N(3)–O(7)	119.8(2)	119(1)	119(1)
O(8)–N(4)–O(9)	119.4(2)	119(1)	120(1)
O(4)–N(5)–O(5)	119.7(2)	117(1)	116(1)

^a X represents a nitrogen atom in the nitrosyl geometry and an oxygen atom in the isonitrosyl structure.

A decrease in the $\angle \text{Ru}(\text{N}–\text{O})$ angle from 174.0(2) to 169(1)^o is observed. The tendency for such bending has been observed previously for SNP and was explained by a lifting of

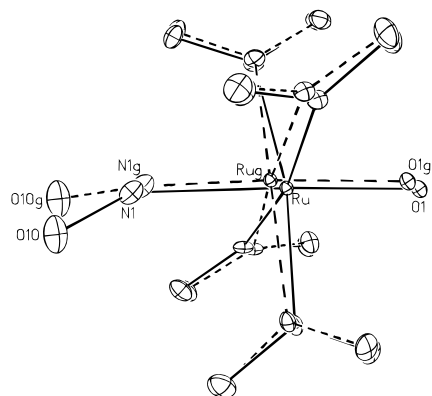


Figure 5. Changes of the structure of the $[\text{Ru}(\text{NO}_2)_4(\text{OH})(\text{NO})]^{2-}$ anion upon excitation: dashed lines, ground state; full lines, excited state. For illustration purposes, all changes have been magnified by a factor 5.

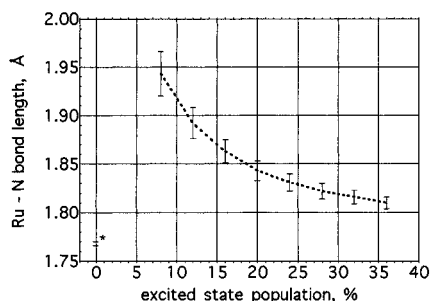


Figure 6. Ru-N bond length *vs* excited state population used in the refinement of the excited-state structure. The * in the lower left corner marks the ground-state bond length.

the degeneracy of the 7e level, antibonding with respect to the M-N and N-O bonds, as a result of a Jahn-Teller distortion arising from the population of a degenerate electronic state.⁴

An elongation of the N-O bond, expected from the shift of the stretching frequency of (NO) from 1886 to 1772 cm^{-1} in MS_1 , was not observed either in SNP or in the present study, even though Badger's rule²³ has been used to predict a change of 0.024 Å upon excitation.²⁴ Either Badger's rule is not applicable in this case, or the shift must be explained in an alternate way.

New Interpretation of the MS_1 Excited State. Though the excited states of the nitrosyl complexes have been described as electronically-excited states in the literature, there is an alternative explanation which is supported by our experiments. When the excited-state refinement is modified by allowing variation of isotropic temperature parameters of the excited-state N and O atoms of the nitrosyl group, the value for oxygen is found to be more than 4 times that of the nitrogen atom, indicating that the scattering power of the proximal atom of the nitrosyl group is underestimated and/or that of the terminal atom is overestimated. In an anisotropic refinement, excited-state nitrosyl nitrogen thermal parameters become nonpositive definite. However, an interchange of N and O produces very reasonable mean-square displacements, with the terminal N atom having a mean-square displacement comparable to that of the oxygen terminal atom in the ground state, as given in Table 5 and illustrated in Figure 7.

The same indication is obtained by examination of the peak heights in a difference Fourier map in which the 84% ground-

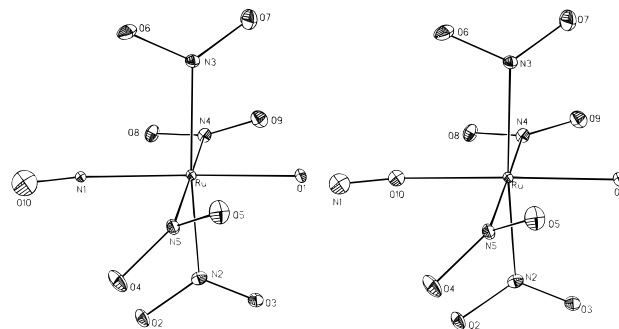


Figure 7. ORTEP drawings of the Ru-NO (left) and Ru-ON (right) models for the MS_1 excited state, showing the differences in the nitrosyl thermal parameters. Thermal parameters for the other atoms are the same as those for the ground-state molecules. 50% probability ellipsoids are shown. The hydroxyl hydrogen atom has been omitted.

Table 5. Isotropic "Thermal" Mean-Square Displacements (\AA^2) for Nitrosyl Atoms in the Excited State for the Ru-NO and Ru-ON Models

atom	ground state	excited state	
		Ru-NO	Ru-ON
N	0.0072(5)	0.0037(13)	0.015(2)
O	0.0141(5)	0.022(2)	0.008(1)

state component of the anion and both cations are subtracted from the total density. The peak heights at the proximal and terminal atom of the nitrosyl group are 1.62 and 1.24 $\text{e}\text{\AA}^3$, respectively, indicating the atom closest to Ru to have the larger atomic number. These results imply that the first metastable state is a geometrical isomer in which the NO group is inverted relative to the ground-state structure. Evidence supporting this conclusion comes from both the X-ray and neutron studies on sodium nitroprusside (SNP) and is briefly summarized here: (a) the valence-shell populations obtained in an electron density refinement of the excited state using 138 K data, reported earlier,⁴ show valence-electron populations of 5.9(3) on the proximal and 5.0(4) on the distal atom, opposite to what is found for the ground state;⁴ (b) as in the current study, for the excited state of SNP, but not for the ground state, the peak heights in a difference map are higher for the proximal atom than for the terminal atom;⁵ and (c) as in the current study, the anomaly for the mean-square vibrations of the excited-state nitrosyl atoms disappears when the isonitrosyl geometry is adopted.⁵ On the other hand, in a previous neutron diffraction study based on the nitrosyl geometry, the thermal parameters of the excited-state species are reported to be *higher* for the proximal than for the terminal (NO) atom, indicating that the scattering power of the distal atom had been *overestimated*.^{3,24} Since the neutron scattering amplitude for N ($b = 9.36 \text{ fm}$) is larger than for O ($b = 5.80 \text{ fm}$),²⁵ the result is readily understood in view of the isonitrosyl geometry of MS_1 and thus confirms the conclusions of the X-ray studies.

Bond lengths and angles for the isonitrosyl structure have been included in Table 4. We note that the observed decrease of the NO stretching frequency by 114 cm^{-1} ,¹⁰ referred to above, is similar to that observed for the analogous isomerization of trimethylsilyl cyanide to trimethylsilyl isocyanide²⁶ and thus is in agreement with the linkage-isomer concept.

The change in metal-nitrosyl ligand distance upon light irradiation is in the direction expected on the basis of linkage isomerism. While the shortest Ru-(two-coordinate N) distances

(23) Hershbach, D. R.; Laurie, V. W. *J. Solid State Phys.* **1961**, *35*, 458-463.

(24) Rüdinger, M.; Schefer, J.; Chevrier, G.; Furer, N.; Gudel, H. U.; Haussühl, S.; Heger, G.; Schweiss, P.; Vogt, T.; Woike, Th.; Zöllner, H. *Z. Phys.* **1991**, *B83*, 125-130.

(25) *International Tables for Crystallography*; Kluwer: Dordrecht, 1992; Vol. C, p 384.

(26) Booth, M. R.; Frankiss, G. S. *Spectrochim. Acta* **1970**, *26A*, 859-869.

in the compounds listed in the Cambridge Structural Data Base cluster around 1.74 Å, the shortest comparable Ru–O distances are typically 1.88 Å, which indicates that the Ru–O distance of the inverted model falls in an acceptable range of distances between the two atoms.

Finally, we note for completeness that our analysis of the excited states of SNP shows the second metastable state of SNP to be a linkage isomer with a side-bound nitrosyl group, again in accordance with the linkage-isomer concept supported by the present study.⁵

Concluding Remarks

The geometry changes upon excitation of $K_2[Ru(NO_2)_4(OH)(NO)]$ are qualitatively the same as those observed for sodium nitroprusside, but with a significantly larger elongation of the M–NO (M = Fe, Ru) distance. As for sodium nitroprusside, the X-ray analysis provides evidence that the first photoinduced metastable state of the transition metal nitrosyl complexes is not an electronically excited state as generally assumed but is

rather a geometric isomer formed by recombination of an initially dissociated nitrosyl group. This model also gives an explanation for the unusually long lifetime of the metastable state, which cannot be understood on the basis of the small geometry changes alone.

Acknowledgment. We thank Dr. M. R. Pressprich for help with initiating the experiments, Dr. R. Bolotovskiy for assistance with the processing of the data, and Dr. M. Carducci for stimulating discussions. Support of this work by the National Science Foundation (Grant CHE9317770) and the donors of the Petroleum Research Fund, administered by the American Chemical Society (Grant PRF28664-AC3), is gratefully acknowledged.

Supporting Information Available: Listings of anisotropic thermal parameters for the ground state structure and structure factor statistics for the both ground- and excited-state data sets (3 pages). Ordering information is given on any current masthead page.

IC9607144